Scalar perturbations in braneworld cosmology

Antonio Cardoso,[1,*] Takashi Hiramatsu,[2,†] Kazuya Koyama,[1,‡] and Sanjeev S. Seahra[1,§]

[1] *Institute of Cosmology & Gravitation, University of Portsmouth, Portsmouth PO1 2EG, UK*
[2] *Research Center for the Early Universe (RESCEU), School of Science, University of Tokyo, 7-3-1 Hongo, Bunkyo, Tokyo 113-0033, Japan*

(Dated: May 11, 2007)

We study the behaviour of scalar perturbations in the radiation-dominated era of Randall-Sundrum braneworld cosmology by numerically solving the coupled bulk and brane master wave equations. We find that density perturbations with wavelengths less than a critical value (set by the bulk curvature length) are amplified during horizon re-entry. This means that the radiation era matter power spectrum will be at least an order of magnitude larger than the predictions of general relativity (GR) on small scales. Conversely, we explicitly confirm from simulations that the spectrum is identical to GR on large scales. Although this magnification is not relevant for the cosmic microwave background or measurements of large scale structure, it will have some bearing on the formation of primordial black holes in Randall-Sundrum models.

I. INTRODUCTION

Our view of cosmology has been revolutionized by the notion that the universe may be a lower-dimensional object embedded in some higher-dimensional space. A particularly simple realization of this idea is furnished by the Randall-Sundrum (RS) braneworld model [1], which postulates that our observable universe is a thin 4-dimensional hypersurface residing in 5-dimensional anti-de Sitter (AdS) space (see Refs. [2, 3, 4] for reviews). Ordinary matter degrees of freedom are assumed to be confined to the brane, while gravitational degrees of freedom are allowed to propagate in the full 5-dimensional bulk. The warping of AdS space allows us to recover ordinary general relativity (GR) at distances greater than the curvature radius of the bulk ℓ. Current laboratory tests of Newton's law constrain ℓ to be less than around 0.1 mm [5].

The cosmological implications of the Randall-Sundrum scenario have been extensively studied. It is well known that the Friedmann equation governing the expansion of the brane universe differs from general relativity by a correction of order ρ/σ, where ρ is the density of brane matter and $\sigma \gtrsim (\text{TeV})^4$ is the brane tension. The magnitude of this correction defines the "high-energy" regime of braneworld cosmology as the era when $\rho \gtrsim \sigma$ or equivalently $H\ell \gtrsim 1$, where H is the Hubble parameter. At high energies, the RS Friedmann equation implies $H \propto \rho$, which results in dynamics significantly different from the standard $H^2 \propto \rho$ expansion law.

The major outstanding issue in RS cosmology is the behaviour of cosmological perturbations [6, 7, 8, 9, 10]. The equations of motion governing fluctuations of the model are found to differ from GR in two principal ways at early times: First, they acquire $\mathcal{O}(\rho/\sigma)$ high-energy corrections similar to those found in the Friedmann equation. By themselves, such corrections are not difficult to deal with: they just modify the second-order ordinary differential equations (ODEs) governing perturbations in GR. But the second type of modification is more problematic: Perturbations on the brane are also coupled to fluctuations of the 5-dimensional bulk geometry, which are collectively known as the "Kaluza Klein" (KK) degrees of freedom of the model. The KK modes are governed by master partial differential equations (PDEs) defined throughout the AdS bulk [6, 7]. In the original work of Randall & Sundrum [1], the brane had a simple Minkowski geometry and the KK mode master wave equations were solvable via separation of variables. But the motion of the brane in the cosmological case breaks the time-translation symmetry of the bulk, which makes a simple separable solution unattainable in most cases. The exception is the case of a brane undergoing de Sitter inflation, where many analytic and semi-analytic results are now available [11, 12, 13, 14, 15].

Many authors have considered various schemes to solve the perturbation problem without dealing with the KK master PDEs directly. The most straightforward approach is to simply set the KK degrees of freedom to zero while retaining $\mathcal{O}(\rho/\sigma)$ corrections, which we refer to as the "4-dimensional effective theory". There are several approximation methods that attempt to move beyond this simplest effective theory in the case of tensor and scalar

*Electronic address: antonio.cardoso.AT.port.ac.uk
†Electronic address: hiramatsu.AT.resceu.s.u-tokyo.ac.jp
‡Electronic address: kazuya.koyama.AT.port.ac.uk
§Electronic address: sanjeev.seahra.AT.port.ac.uk

perturbations [16, 17, 18, 19, 20, 21, 22, 23, 24, 25, 26, 27]. These generally consider the behaviour of fluctuations during certain limiting regimes (i.e, high-energy or low-energy), but the only known way of tackling the problem on all scales simultaneously is by direct numerical solution of the equations of motion.

The problem of tensor perturbations is somewhat simpler than the scalar case. The reason is that in linear theory, tensor modes are pure gravitational degrees of freedom that do not couple to matter fluctuations (provided that the matter anisotopic stress is neglected). In the braneworld context, this means that there are no brane-confined tensor degrees of freedom. The perturbation problem formally reduces to solving a wave equation in the bulk with boundary conditions imposed on a moving brane. Numeric solutions have been obtained by several groups [28, 29, 30, 31, 32, 33, 34, 35]. Interestingly, the effective theory predicts a blue spectrum (i.e. excess power) in the stochastic gravitational wave background at frequencies corresponding to modes that enter the Hubble horizon in the high-energy regime. However, once KK effects are incorporated via numeric simulations, one finds that the true spectrum is flat and virtually identical to GR. That is, the magnitudes of the $\mathcal{O}(\rho/\sigma)$ and KK effects are nearly the same, but they act in opposite sense and end up canceling each other out. Physically, the reason that the KK modes cause a suppression of the amplitude at high frequencies is that they efficiently radiate gravitational wave energy from the brane into the bulk.

The purpose of the paper is to numerically solve for the behaviour of scalar perturbations in the radiation-dominated regime of braneworld cosmology. (Numeric analysis of the scalar perturbations during inflation has already been done in Refs. [13, 15].) Unlike the tensor case, there are several scalar degrees of freedom residing on the brane, such as the density contrast $\delta\rho/\rho$. The problem reduces to the solution of a bulk wave equation coupled to a master boundary field satisfying its own second order ODE on the moving brane. Recently, two of the numerical codes developed to deal with tensor perturbations [28, 35] have been generalized to handle boundary degrees of freedom [13, 36]. We use both codes in this paper, which gives us the ability to confirm the consistency of our numeric results via two independent algorithms. We are ultimately interested in finding the matter transfer function in the radiation era, and also determining the relative influence of KK and high-energy effects on the density perturbations. Heuristically, we may expect the KK modes to amplify high-energy/small-scale density perturbations, which is the opposite effect from the tensor case. The reason is that we know that the gravitational force of attraction in the RS model is stronger than in GR on scales less than ℓ [1, 37]. This implies that modes with a physical wavelength smaller than ℓ during horizon crossing will be amplified due to the KK enhancement of the gravitational force. However, this physical reasoning needs to be tested with numeric simulations.

The layout of the paper is as follows: The background geometry of the RS cosmology we consider is described in §II. The formulae governing the gauge invariant scalar perturbations are given in §III. Also in that section, we derive new analytic approximations for various perturbation variables at very high energies. In §IV, we present the numeric algorithms that we use to solve the coupled system of bulk and brane wave equations. Our results for the matter transfer function are also contained in that section. Finally, we summarize and discuss the implications of our work in §V

II. BACKGROUND GEOMETRY AND BRANE DYNAMICS

As discussed in the Introduction, the Randall-Sundrum model we will be considering consists of a thin brane, which is realized as singular 4-surface, residing in 5-dimensional anti-de Sitter space. In Poincaré coordinates, the bulk metric is given by the line element

$$ds_5^2 = \frac{\ell^2}{z^2}(-d\tau^2 + \delta_{ij}dx^i dx^j + dz^2). \tag{1}$$

Here, ℓ is the curvature scale of the bulk. The boundary of this spacetime given by a brane is described parametrically by

$$\tau = \tau_{\rm b}(\eta), \quad z = z_{\rm b}(\eta). \tag{2}$$

The parameter η is defined to be the conformal time along the brane, which leads to the following induced line element

$$d\eta^2 = d\tau_{\rm b}^2 - dz_{\rm b}^2, \quad ds_{\rm b}^2 = a^2(-d\eta^2 + d\mathbf{x}^2) = -dt^2 + a^2 d\mathbf{x}^2. \tag{3}$$

Here, we have identified the scale factor as $a(\eta) = \ell/z_{\rm b}(\eta)$ and t as the cosmic time. Now, we define $u^a = dx^a_{\rm b}/dt$ to be the 5-velocity field of comoving observers on the brane, while n^a is the brane normal. These vector fields can then

be used to construct directional derivatives parallel and orthogonal to the brane:

$$\partial_u = u^a\partial_a = \frac{1}{a}\left(\sqrt{1+H^2\ell^2}\,\frac{\partial}{\partial\tau} - H\ell\frac{\partial}{\partial z}\right) = \frac{\partial}{\partial t} = \frac{1}{a}\frac{\partial}{\partial\eta}, \tag{4a}$$

$$\partial_n = n^a\partial_a = \frac{1}{a}\left(-H\ell\frac{\partial}{\partial\tau} + \sqrt{1+H^2\ell^2}\,\frac{\partial}{\partial z}\right), \tag{4b}$$

respectively. Here, H is the usual Hubble parameter

$$H = \left(\frac{\partial_u r}{r}\right)_{\rm b} = \frac{1}{a}\frac{da}{dt}, \quad \frac{r}{\ell} = \frac{\ell}{z}, \tag{5}$$

where we have introduced the alternative bulk coordinate r. We assume that the matter on the brane has a fluid-like stress-energy tensor with density ρ and pressure p:

$$T_{ab} = (\rho+p)u_a u_b + p h_{ab}, \quad g_{ab} = h_{ab} + n_a n_b. \tag{6}$$

The junction conditions are given in terms of the extrinsic curvature K_{ab} of the brane,

$$K_{ab} = h_a{}^c\nabla_c n_b, \qquad 2K_{ab} = -\kappa_5^2[T_{ab} - \tfrac{1}{3}h_{ab}(T-\sigma)], \tag{7}$$

where $\kappa_5^2 = 1/M_5^3$ is the gravity-matter coupling in 5 dimensions and σ is the brane tension. This yields

$$\left(\frac{\partial_n r}{r}\right)_{\rm b} = -\frac{\kappa_5^2(\rho+\sigma)}{6} = -\frac{\sqrt{1+H^2\ell^2}}{\ell}. \tag{8}$$

We assume the standard Randall-Sundrum fine-tuning

$$\kappa_5^2 = \kappa_4^2\ell = 8\pi G\ell = \frac{6}{\sigma\ell}, \tag{9}$$

to obtain the Friedmann equation

$$H^2 = \frac{1}{\ell^2}\frac{\rho}{\sigma}\left(2+\frac{\rho}{\sigma}\right) = \frac{8\pi G}{3}\rho\left(1+\frac{\rho}{2\sigma}\right). \tag{10}$$

Note the high-energy $\mathcal{O}(\rho/\sigma)$ correction to the expansion rate. Finally, note that we have the usual conservation of stress-energy on the brane; i.e.,

$$h^{ab}\nabla_a T_{bc} = 0, \qquad \frac{d\rho}{dt} = -3(1+w)\rho H, \qquad w = \frac{p}{\rho}. \tag{11}$$

III. SCALAR PERTURBATIONS

A. Gauge invariant bulk perturbations

We now turn our attention to the perturbation of the cosmology introduced in §II. It has been shown in Refs. [6, 7] that scalar-type perturbations of the bulk geometry (1) are governed by a single gauge invariant master variable Ω. We summarize those results in this subsection.

First, we introduce a harmonic basis with mode functions[1]

$$Y = e^{i\mathbf{k}\cdot\mathbf{x}}, \qquad Y_i = -\frac{1}{k}\partial_i Y, \qquad Y_{ij} = \frac{1}{k^2}\partial_i\partial_j Y + \frac{1}{3}\delta_{ij}Y. \tag{12}$$

[1] To describe the perturbations in the RS model we mostly follow the notation and conventions of Kodama et al. [7], which are based on the 4-dimensional formalism of Kodama and Sasaki [38].

Using these mode functions, we write the perturbed bulk metric as

$$ds_5^2 = (q_{\alpha\beta} + f_{\alpha\beta})dx^\alpha dx^\beta + \frac{2r}{\ell} f_\alpha Y_i dx^\alpha dx^i + \frac{r^2}{\ell^2}\left[(1+2H_L)\delta_{ij} + 2H_T Y_{ij}\right] dx^i dx^j, \tag{13}$$

where

$$q_{\alpha\beta}dx^\alpha dx^\beta = \frac{\ell^2}{z^2}(-d\tau^2 + dz^2). \tag{14}$$

Implicit integration over the wavevector $\mathbf{k}$ is understood in equations like (13). A priori, the particular form of the perturbation variables $f_{\alpha\beta}$, f_α, H_L and H_T depend on the choice of gauge. However, one can construct gauge invariant combinations as follows

$$F = H_L + \frac{1}{3}H_T + \frac{X^\alpha D_\alpha r}{r}, \qquad F_{\alpha\beta} = f_{\alpha\beta} + D_\alpha X_\beta + D_\beta X_\alpha, \tag{15}$$

where

$$X_\alpha = \frac{r}{k\ell}\left(f_\alpha + \frac{r}{k\ell} D_\alpha H_T\right), \tag{16}$$

and D_α is the covariant derivative associated with the 2-metric $q_{\alpha\beta}$. The gauge invariant quantities are then given in terms of the master variable $\Omega = \Omega(t,z)$

$$F = \frac{1}{6r}\left(D^\mu D_\mu - \frac{2}{\ell^2}\right)\Omega, \quad F_{\alpha\beta} = \frac{1}{r}\left[D_\alpha D_\beta - \frac{1}{3}q_{\alpha\beta}\left(2D^\mu D_\mu - \frac{1}{\ell^2}\right)\right]\Omega. \tag{17}$$

The bulk master variable satisfies the following wave equation

$$0 = -\frac{\partial^2\Omega}{\partial\tau^2} + \frac{\partial^2\Omega}{\partial z^2} + \frac{3}{z}\frac{\partial\Omega}{\partial z} + \left(\frac{1}{z^2} - k^2\right)\Omega. \tag{18}$$

B. Gauge invariant brane perturbations

In addition to perturbations of the bulk metric, we must also consider perturbations of the brane metric. These are parameterized as

$$ds_{\rm b}^2 = (1-2\alpha Y)dt^2 - 2a\beta Y_i dt\, dx^i + a^2\left[(1+2h_L)\delta_{ij} + 2h_T Y_{ij}\right] dx^i dx^j. \tag{19}$$

As in 4 dimensions, the gauge-dependant variables $(\alpha, \beta, h_L, h_T)$ can be used to construct gauge-invariant quantities

$$\Phi = h_L + \frac{1}{3}h_T - \frac{Ha}{k}\sigma_g, \qquad \Psi = \alpha - \frac{1}{k}\frac{d}{dt}(a\sigma_g), \tag{20}$$

where

$$\sigma_g = \frac{a}{k}\frac{dh_T}{dt} - \beta. \tag{21}$$

As demonstrated in Ref. [39], the effective Einstein equation on the brane is in general given by

$${}^{(4)}G_{ab} = \kappa_4^2 T_{ab} + \kappa_5^2 \Pi_{ab} - \mathcal{E}_{ab}, \qquad \Pi_{ab} = -\frac{1}{4}T_{ac}T^c{}_b + \frac{1}{12}TT_{ab} + \frac{1}{8}T_{cd}T^{cd}h_{ab} - \frac{1}{24}T^2 h_{ab}. \tag{22}$$

Here, $\mathcal{E}_{ab}$ represents the projection of the electric part of the bulk Weyl tensor onto the brane. Notice that $\mathcal{E}_{ab}$ satisfies

$$h^{ab}\mathcal{E}_{ab} = 0, \qquad \nabla_a(\kappa_5^2\Pi^{ab} - \mathcal{E}^{ab}) = 0, \tag{23}$$

and vanishes in the background geometry discussed in §II. When perturbing (22), one can treat $\mathcal{E}_{ab}$ as an additional fluid source with a radiation-like equation of state. Hence, we parameterize the perturbations of T_{ab} and $\mathcal{E}_{ab}$ as

$$\delta T_0{}^0 = -\delta\rho\, Y, \qquad \delta\mathcal{E}_0{}^0 = \kappa_4^2\delta\rho_{\mathcal{E}} Y, \tag{24a}$$

$$\delta T_i{}^0 = -kY_i\delta q, \qquad \delta\mathcal{E}_i{}^0 = \kappa_4^2 kY_i\delta q_{\mathcal{E}}, \tag{24b}$$

$$\delta T_i{}^j = \delta p Y\delta_i{}^j + k^2\delta\pi Y_i{}^j, \qquad \delta\mathcal{E}_i{}^j = -\kappa_4^2(\tfrac{1}{3}\delta\rho_{\mathcal{E}} Y\delta_i{}^j + k^2\delta\pi_{\mathcal{E}} Y_i{}^j). \tag{24c}$$

Henceforth, we will assume that the matter anisotropic stress vanishes $\delta\pi = 0$. The Weyl fluid perturbations $(\delta\rho_{\mathcal{E}}, \delta q_{\mathcal{E}}, \delta\pi_{\mathcal{E}})$ are the "Kaluza-Klein" (KK) degrees of freedom of the model alluded in the Introduction, since they represent the effects of bulk geometry fluctuations on the brane. The matter perturbation variables above are not gauge invariant, but the following quantities are:

$$\rho\Delta = \delta\rho - 3H\delta q, \qquad a(\rho+p)V = -k\delta q - (\rho+p)a\sigma_g, \qquad \Gamma = \delta p - c_s^2\delta\rho, \tag{25a}$$

$$\rho\Delta_{\mathcal{E}} = \delta\rho_{\mathcal{E}} - 3H\delta q_{\mathcal{E}}, \qquad a(\rho+p)V_{\mathcal{E}} = -k\delta q_{\mathcal{E}} - (\rho+p)a\sigma_g. \tag{25b}$$

Here, we have defined the sound speed as $c_s^2 = \delta p/\delta\rho$. Since the Weyl fluid has the equation of state $\delta p_{\mathcal{E}} = \frac{1}{3}\delta\rho_{\mathcal{E}}$, there is no KK entropy perturbation $\Gamma_{\mathcal{E}} = 0$. Furthermore, the KK anisotropic stress is automatically gauge invariant. Armed with these definitions, it is possible to derive the following gauge-invariant equations from the perturbation of Eq. (22):

$$\Phi = \frac{4\pi G\rho a^2}{k^2}\left[\left(1+\frac{\rho}{\sigma}\right)\Delta + \Delta_{\mathcal{E}}\right], \tag{26a}$$

$$H\Psi - \frac{d\Phi}{dt} = \frac{4\pi G(\rho+p)a}{k}\left[\left(1+\frac{\rho}{\sigma}\right)V + V_{\mathcal{E}}\right], \tag{26b}$$

$$\Phi + \Psi = -8\pi G a^2\delta\pi_{\mathcal{E}}. \tag{26c}$$

The first of these gives the high-energy $\mathcal{O}(\rho/\sigma)$ and KK corrections to the Poisson equation on the brane. The second equation gives the modifications of the standard equation governing the evolution of the peculiar velocity field. The third equation demonstrates how the KK-modes can give rise to an anisotropic stress on the brane.

Additional equations can be obtained from perturbing the equation representing the conservation of matter stress energy on the brane: $\delta(h^{ab}\nabla_a T_{bc}) = 0$. These are

$$\frac{1}{a}\frac{d}{dt}(aV) = \frac{k}{a}\Psi + \frac{k}{a}\frac{\Gamma + c_s^2\rho\Delta}{\rho(1+w)}, \tag{27a}$$

$$\frac{1}{a^3}\frac{d}{dt}(a^3\rho\Delta) = -\frac{k}{a}\rho(1+w)\left(1 - \frac{3a^2}{k^2}\frac{dH}{dt}\right)V - 3\rho(1+w)\left(\frac{d\Phi}{dt} - H\Psi\right). \tag{27b}$$

Finally, we can also perturb the righthand expression in Eq. (23) to get two more equations, but these are not sufficient to close the effective Einstein equations (22) on the brane. Hence we can only go so far with this effective Weyl fluid description; a complete treatment must describe how the brane degrees of freedom presented here are coupled to the bulk degree of freedom Ω.

C. Perturbation of the junction conditions

The means to connect the bulk perturbations of §III A and the brane perturbations of §III B is the perturbation of the junction conditions (7). This yields several results, the most important of which is that Ω satisfies a boundary condition on the brane

$$\left[\partial_n\Omega + \frac{1}{\ell}\left(1+\frac{\rho}{\sigma}\right)\Omega + \frac{6\rho a^3}{\sigma k^2}\Delta\right]_{\rm b} = 0. \tag{28}$$

The perturbation of (7) also gives the KK gauge invariants in terms of Ω:

$$\kappa_4^2\rho\Delta_{\mathcal{E}} = \frac{k^2}{\ell a^3}\left[\frac{k^2+3H^2a^2}{3a^2}\Omega - H\partial_u\Omega\right]_{\rm b}, \tag{29a}$$

$$\kappa_4^2 a(\rho+p)V_{\mathcal{E}} = \frac{k^3}{3\ell a^2}\left[H\Omega - \partial_u\Omega\right]_{\rm b}, \tag{29b}$$

$$\kappa_4^2\delta\pi_{\mathcal{E}} = \frac{1}{2\ell a^3}\left[\frac{1}{3}k^2\Omega - H\partial_u\Omega - \frac{3(\rho+p)}{\ell\sigma}\partial_n\Omega + \partial_u^2\Omega\right]_{\rm b}. \tag{29c}$$

These reproduce the results first derived in Ref. [40]. Using these equations, we can find explicit formulae for the gauge invariants defined above in terms of Δ and $\Omega_{\rm b}(\eta) = \Omega(\tau_{\rm b}(\eta), z_{\rm b}(\eta))$:

$$\Phi = \frac{3a^2\rho(\rho+\sigma)}{k^2\ell^2\sigma^2}\Delta + \left(\frac{3H^2a^2+k^2}{6\ell a^3}\right)\Omega_{\rm b} - \frac{H}{2\ell a^2}\frac{d\Omega_{\rm b}}{d\eta}, \tag{30a}$$

$$\Psi = -\frac{3\rho a^2(3w\rho+4\rho+\sigma)}{k^2\ell^2\sigma^2}\Delta - \left[\frac{(3w+4)\rho^2}{2\ell^3 a\sigma^2} + \frac{(5+3w)\rho}{2\ell^3 a\sigma} + \frac{k^2}{3\ell a^3}\right]\Omega_{\rm b} + \frac{3H}{2\ell a^2}\frac{d\Omega_{\rm b}}{d\eta} - \frac{1}{2\ell a^3}\frac{d^2\Omega_{\rm b}}{d\eta^2}, \tag{30b}$$

$$V = \frac{3wHa}{k(1+w)}\Delta - \frac{1}{k(1+w)}\frac{d\Delta}{d\eta} + \frac{kH}{2\ell a^2}\Omega_{\rm b} - \frac{k}{2\ell a^3}\frac{d\Omega_{\rm b}}{d\eta}. \tag{30c}$$

Other quantities of interest are the curvature perturbation on uniform density slices,

$$\zeta = \Phi - \frac{HaV}{k} + \frac{\Delta}{3(1+w)} = \left[\frac{1}{3} - \frac{3\rho a^2(w\sigma-\sigma-\rho)}{k^2\ell^2\sigma^2}\right]\frac{\Delta}{1+w} + \frac{Ha}{k^2(1+w)}\frac{d\Delta}{d\eta} + \frac{k^2}{6\ell a^3}\Omega_{\rm b}, \tag{31}$$

and the curvature perturbation on comoving slices,

$$\mathcal{R}_c = \Phi - \frac{HaV}{k} = -\frac{3\rho a^2(w\sigma-\sigma-\rho)}{k^2\ell^2\sigma^2}\frac{\Delta}{1+w} + \frac{Ha}{k^2(1+w)}\frac{d\Delta}{d\eta} + \frac{k^2}{6\ell a^3}\Omega_{\rm b}, \tag{32}$$

Hence, if we have knowledge of the density contrast Δ and the value of Ω on the brane, we can obtain the behaviour of all the other gauge invariants via algebra and differentiation.

The above formulae can be easily manipulated to find a wave equation for Δ:

$$\frac{d^2\Delta}{d\eta^2} + (1+3c_s^2-6w)Ha\frac{d\Delta}{d\eta} + \left[c_s^2k^2 + \frac{3\rho a^2}{\sigma\ell^2}A + \frac{3\rho^2a^2}{\sigma^2\ell^2}B\right]\Delta = -\frac{k^2\Gamma}{\rho} + \frac{k^4(1+w)\Omega_{\rm b}}{3\ell a^3}, \tag{33a}$$

$$A = 6c_s^2 - 1 - 8w + 3w^2, \qquad B = 3c_s^2 - 9w - 4. \tag{33b}$$

The above ODE, the bulk wave equation (18) and the boundary condition (28) comprise a closed set of equations for Δ and Ω.

Before moving on, we have three remarks: First, note that in the low energy universe, we can neglect $\mathcal{O}(\rho^2/\sigma^2)$ terms. Then, the Δ wave equation reduces to

$$\frac{d^2\Delta}{d\eta^2} + (1+3c_s^2-6w)Ha\frac{d\Delta}{d\eta} + \left[c_s^2k^2 + 4\pi G\rho a^2(6c_s^2-1-8w+3w^2)\right]\Delta \approx -\frac{k^2\Gamma}{\rho} + \frac{k^4(1+w)\Omega_{\rm b}}{3\ell a^3}. \tag{34}$$

Setting $\Omega_{\rm b} = 0$ yields the standard 4-dimensional dynamical equation for Δ; hence, we recover GR at low energies. Second, we note that from the conservation of stress-energy on the brane (27), we must have

$$\frac{d\zeta}{d\eta} = -\frac{kV}{3} - \frac{Ha\Gamma}{\rho(1+w)}. \tag{35}$$

We can easily verify that Eqns. (30c), (31) and (33) imply that (35) is satisfied identically, which is a good consistency check of our formulae. Finally, the entropy perturbation can be simplified when the brane matter is either a perfect fluid or a scalar field:

$$\Gamma = (\Upsilon - c_s^2)\rho\Delta, \quad \Upsilon = \begin{cases} c_s^2, & \text{perfect fluid,} \\ 1, & \text{scalar field.} \end{cases} \tag{36}$$

For the rest of this paper, we will be considering the perfect fluid case.

D. Asymptotic behaviour in the high-energy radiation-dominated regime

To model the perturbations in the very early universe, we assume radiation domination and $\rho \gg \sigma$; or, equivalently, $H\ell \gg 1$. Under these circumstances, the following approximations hold:

$$w = 1/3, \quad a \approx a_0(k\eta)^{1/3}, \quad \rho \approx \sigma H\ell, \quad \partial_n \approx -\partial_u = -\partial_t. \tag{37}$$

The last relationship can be used to re-cast the boundary condition on the bulk master variable Ω into a 1st order ordinary differential equation for $\Omega_{\rm b}$. Hence, the equation of motion for Δ and boundary condition become

$$0 \approx \frac{d^2\Delta}{d\eta^2} + \left(\frac{k^2}{3} - \frac{4a_0k^{1/3}}{3\ell\eta^{2/3}} - \frac{2}{\eta^2}\right)\Delta - \frac{4k^3}{9\ell a_0^3\eta}\Omega_{\rm b}, \quad \frac{d\Omega_{\rm b}}{d\eta} \approx \frac{1}{3\eta}\left(1 + \frac{3a_0k^{1/3}\eta^{4/3}}{\ell}\right)\Omega_{\rm b} + \frac{2\ell a_0^3}{k}\Delta. \tag{38}$$

By differentiating the first equation we can derive a decoupled third order equation for Δ, which can be solved via power series methods. The solutions for Δ and Ω are a superposition of three linearly independent modes:

$$\Delta = \sum_{i=1}^{3}\mathcal{A}_i\Delta^{(i)}, \quad \Omega_{\rm b} = \sum_{i=1}^{3}\mathcal{A}_i\Omega_{\rm b}^{(i)}, \tag{39}$$

where the $\mathcal{A}_i$ are constants. At leading order in $(k\eta)$, these mode functions are given by

$$\text{dominant growing mode:} \qquad \Delta^{(1)} \approx \tfrac{4}{3}(k\eta)^2, \qquad \Omega_{\rm b}^{(1)} \approx a_0^3k^{-2}\ell(k\eta)^3, \tag{40a}$$

$$\text{subdominant growing mode:} \qquad \Delta^{(2)} \approx (k\eta)^{4/3}, \qquad \Omega_{\rm b}^{(2)} \approx -\tfrac{7}{2}a_0^3k^{-2}\ell(k\eta)^{1/3}, \tag{40b}$$

$$\text{decaying mode:} \qquad \Delta^{(3)} \approx \tfrac{10}{3}k\ell a_0^{-1}(k\eta)^{-1}, \qquad \Omega_{\rm b}^{(3)} \approx -20a_0^2k^{-1}\ell^2. \tag{40c}$$

As the labels on the left suggest, the growth of density perturbations for the dominant growing mode is faster than for the subdominant growing mode on superhorizon scales. The density contrast of the third mode decays in the high-energy regime.

We can calculate the behaviour of ζ and Ψ for the dominant growing mode by substituting the full series solutions for $\Delta^{(1)}$ and $\Omega^{(1)}$ into (30b) and (31), which yields:

$$\zeta^{(1)} \approx 1, \qquad \Psi^{(1)} \approx -4\zeta^{(1)}. \tag{41}$$

We see that the dominant growing mode curvature perturbation and Newtonian potential are conserved on superhorizon scales. Also note that (41) implies

$$\Delta^{(1)} = \frac{4}{27}\left(\frac{k}{Ha}\right)^2\zeta^{(1)}. \tag{42}$$

Eqs. (41) and (42) are similar to the standard superhorizon growing mode results for a radiation dominated universe in general relativity,

$$\Psi_{\rm GR}^{(1)} \approx -\Phi_{\rm GR}^{(1)} \approx -\frac{3(1+w)}{3w+5}\zeta_{\rm GR}^{(1)} = -\frac{2}{3}\zeta_{\rm GR}^{(1)}, \quad \Delta_{\rm GR}^{(1)} \approx \frac{(3w+1)^2(1+w)}{2(3w+5)}\left(\frac{k}{Ha}\right)^2\zeta_{\rm GR}^{(1)} = \frac{4}{9}\left(\frac{k}{Ha}\right)^2\zeta_{\rm GR}^{(1)}, \tag{43}$$

but the numerical factors are different.[2]

Finally, we note that the method described in the subsection fails to yield an approximate solution for the other metric potential $\Phi^{(1)}$. The reason is that when the full series expansions for $\Delta^{(1)}$ and $\Omega_{\rm b}^{(1)}$ are substituted into (30a), the leading order contribution vanishes, leaving a result that is the same order as the error in the original approximations (37). We must therefore rely on numeric simulations to determine the asymptotic behaviour of Φ.

IV. NUMERIC ANALYSIS

A. Dimensionless parameters and integration algorithms

Our goal in the section is the solution of the system comprised of the bulk wave equation (18) and the brane wave equation (33) subject to the boundary condition (28). For the rest of the paper, we will restrict ourselves to the case of

[2] It is interesting to note that it is impossible to find an effective equation of state parameter $w_{\rm eff}$ to make the general GR formulae given in (43) compatible with (41) and (42). Some authors [41] have previously tried to describe the high-energy radiation epoch of RS cosmology with an effective fluid with $w_{\rm eff} = 5/3$, but we see that this would predict $\Delta^{(1)} \approx 24/5(k/Ha)^2\zeta^{(1)}$ and $\Psi^{(1)} \approx -4\zeta^{(1)}/5$, which is in clear conflict with the correct results (41) and (42). This is due to a large Weyl anisotropic stress that modifies the GR relationship between Ψ and Φ.

a radiation-dominated brane with $w = 1/3$. To perform the analysis, it is necessary to make the various quantities in the equations dimensionless. To do so, we define the "*" epoch as the moment in time when a mode with wavenumber k enters the Hubble horizon

$$k = H_* a_*, \qquad H_* = H(\eta_*), \qquad a_* = a(\eta_*), \qquad z_* = z_{\rm b}(\eta_*). \tag{44}$$

Then, we introduce dimensionless/normalized quantities as

$$\hat{\Omega} = \frac{\Omega}{a_* \ell^3}, \qquad \hat{\rho} = \frac{\rho}{\sigma}, \qquad \hat{H} = H\ell, \qquad \hat{k} = \hat{H}_* = \frac{k\ell}{a_*} = k z_* = \sqrt{\hat{\rho}_*(\hat{\rho}_* + 2)}, \qquad \hat{a} = \frac{a}{a_*}. \tag{45}$$

Another important era is the critical epoch when $\hat{H}_c = H_c \ell = 1$ and the radiation density has its critical value $\hat{\rho}_c = \sqrt{2} - 1$. We define the critical epoch as the transition between high and low energy regimes. The ratio of the wavenumber of any given mode to the wavenumber $k_{\rm c} = H_{\rm c} a_{\rm c}$ of the critical mode that enters the horizon at the critical epoch is

$$\frac{k}{k_{\rm c}} = \sqrt{\hat{\rho}_*(\hat{\rho}_* + 2)} \left(\frac{\sqrt{2} - 1}{\hat{\rho}_*} \right)^{1/4}, \tag{46}$$

where $a_{\rm c}$ is the value of the scale factor at the critical epoch. Generally speaking, we call modes with $k > k_{\rm c}$ "supercritical" and modes with $k < k_{\rm c}$ "subcritical". The scale defined by the critical mode in today's universe (with scale factor a_0) is given by

$$\frac{a_0}{k_{\rm c}} = 1.4 \times 10^{12} \left(\frac{\ell}{0.1\,{\rm mm}} \right)^{1/2} \left(\frac{g_{\rm c}}{100} \right)^{1/12} {\rm m}, \tag{47}$$

where $g_{\rm c}$ is the number of relativistic degrees of freedom in the matter sector at the critical epoch. For $\ell = 0.1\,$mm, this corresponds to a scale of ~ 10 astronomical units (AU), which is incredibly tiny by cosmological standards. Finally, if we normalize all coordinates by z_*,

$$\hat{\tau} = \tau / z_*, \quad \hat{z} = z / z_*, \quad \hat{\eta} = \eta / z_*, \tag{48}$$

we find that the entire system of master equations is characterized by the dimensionless matter density at horizon crossing $\hat{\rho}_*$.

Once the system has been reduced into the dimensionless form, we have two independent numerical codes that can be used to solve for Δ and $\hat{\Omega}_{\rm b}$. The first is the pseudo-spectral (PS) method used in Ref. [13, 30] and the second is the characteristic integration (CI) algorithm developed in Ref. [36][3]; detailed descriptions of each method can be found in the respective papers. There is one technical difference between the two algorithms that is worth highlighting here: Namely, each code solves for $\hat{\Omega}$ in different regions of the 5-dimensional spacetime, as shown in Fig. 1. One implication of this is that the initial data for each code needs to be specified at different places. For the PS code, one needs to choose $\hat{\Omega}$ and $\partial\hat{\Omega}/\partial\hat{\tau}$ on an initial spacelike hypersurface $\partial\mathcal{M}^-_{\rm PS}$ of constant $\hat{\tau}$, while for the CI algorithm one needs $\hat{\Omega}$ only on an initial null hypersurface $\partial\mathcal{M}^-_{\rm CI}$ intersecting the brane.

What initial conditions should we actually use? The calculations of §III D suggest that at sufficiently early times, the dynamics of the system are well described by three distinct modes (40). If our initial data surface is positioned within this early era, it follows that generic choices of initial conditions will excite some superposition of these three modes. However, after a short period of time the dominant growing mode will overtake the contributions from the subdominant growing and decaying modes. Hence, we expect that the late time dynamics of our model will be insensitive to the choice of initial conditions, provided that the initial data hypersurface is oriented at an early enough time. Since we do not expect the initial conditions to matter very much, we make the simple choices

$$\text{PS initial conditions:} \quad \Delta(O) = \mathcal{N}\hat{a}_i^6, \quad \hat{\partial}_\eta \Delta(O) = 6\mathcal{N}\hat{H}_i \hat{a}_i^7, \quad \hat{\Omega}(\partial\mathcal{M}^-_{\rm PS}) = 0, \quad \hat{\partial}_\tau \hat{\Omega}(\partial\mathcal{M}^-_{\rm PS}) = 6\mathcal{N}\hat{\rho}_* \hat{a}_i^6 / \hat{k}^2 \hat{H}_i, \tag{49a}$$

$$\text{CI initial conditions:} \quad \Delta(O) = \mathcal{N}\hat{a}_i^6, \quad \hat{\partial}_\eta \Delta(O) = 6\mathcal{N}\hat{H}_i \hat{a}_i^7, \quad \hat{\Omega}(\partial\mathcal{M}^-_{\rm CI}) = 0, \tag{49b}$$

[3] To apply the CI method as described in [36], the bulk wave equation needs to be mapped into a canonical form via the change of variable $\hat{\Omega} = (z_*/z)^{3/2}\phi$.

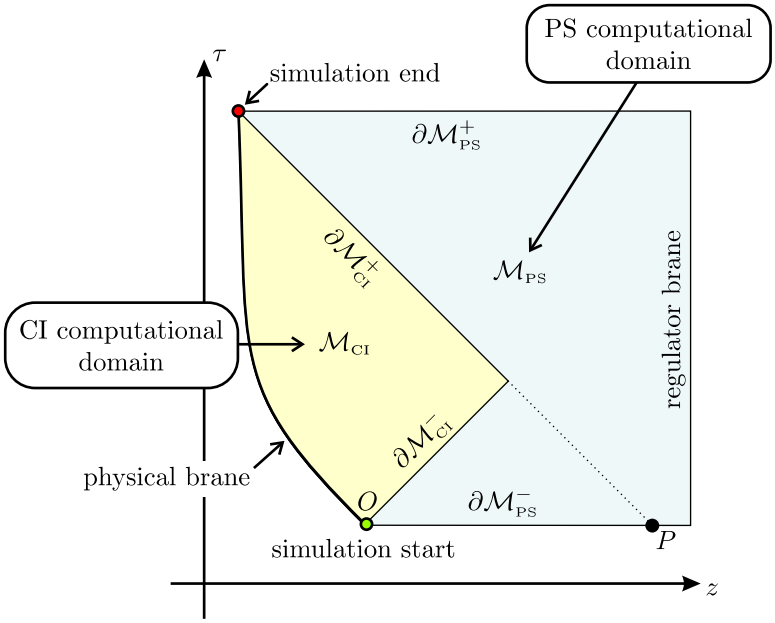

FIG. 1: The computational domains employed by the pseudo-spectral (PS) and characteristic integration (CI) methods. The future and past boundaries $\partial\mathcal{M}^{\pm}_{\rm PS}$ of the PS domain $\mathcal{M}_{\rm PS}$ are lines of constant τ, while for the CI method they are null rays. In the PS method, one needs a constant z regulator brane to render the computational domain finite. In principle, the position of the regulator is free, but it should be placed to the right of the point P in order to be outside the causal past of the physical brane. Initial conditions for the two methods are placed on $\partial\mathcal{M}^-_{\rm PS}$ and $\partial\mathcal{M}^-_{\rm CI}$, respectively.

where $\hat{\partial}_\eta = \partial/\partial\hat{\eta}$, $\hat{\partial}_\tau = \partial/\partial\hat{\tau}$, and an "$i$" subscript denotes the initial value of the scale factor and Hubble parameter. Here, $\mathcal{N}$ is a normalization constant that we will often select to make $\zeta = 1$ at the initial time. These initial conditions are motivated by the fact that we expect $\Delta \propto \hat{a}^6 \gg \hat{\Omega}_{\rm b}$ for the dominant growing mode at very early times, which can certainly be satisfied by setting $\hat{\Omega} = 0$ on the initial data surface. For the PS method, the initial time derivative of $\hat{\Omega}$ is selected to satisfy the boundary condition (28) at the initial time. Note that the initial conditions for the two methods are actually incompatible due to the different locations of the initial surface. But as we have argued above and will see below, this difference should make no difference to the final results. (We will test this assumption in §IV D below.)

B. Typical waveforms

We now turn to the results of our simulations. In Fig. 2 we show the output of the PS and CI codes for a typical simulation of a supercritical mode with $\hat{\rho}_* = 50$. As expected we have excellent agreement between the two codes, despite the fact that they use different initial conditions (49). In fact, we have confirmed that the codes give essentially identical results for a wide range of parameters, which gives us confidence in our numerical methods. It is also reassuring that the simulation results closely match the analytic predictions of §III D on high-energy/superhorizon scales. Note that for all simulations, we recover that Δ and ζ are phase-locked plane waves,

$$\Delta(\eta) \propto \cos\frac{k\eta}{\sqrt{3}}, \quad \Delta(\eta) \approx 4\zeta(\eta), \tag{50}$$

at sufficiently late times $k\eta \gg 1$, which is actually the same behaviour as seen in GR, where we have the following exact solutions for the growing mode density contrast and curvature perturbation during radiation domination:

$$\Delta^{(1)}_{\rm GR} = \mathcal{A}\left(\frac{\sqrt{3}}{k\eta}\sin\frac{k\eta}{\sqrt{3}} - 4\cos\frac{k\eta}{\sqrt{3}}\right) \approx \mathcal{A}\begin{cases}\frac{4}{9}k^2\eta^2, & k\eta \ll 1,\\ -4\cos\frac{k\eta}{\sqrt{3}}, & k\eta \gg 1,\end{cases} \tag{51a}$$

$$\zeta^{(1)}_{\rm GR} = \mathcal{A}\left(\frac{2\sqrt{3}}{k\eta}\sin\frac{k\eta}{\sqrt{3}} - \cos\frac{k\eta}{\sqrt{3}}\right) \approx \mathcal{A}\begin{cases}1, & k\eta \ll 1,\\ -\cos\frac{k\eta}{\sqrt{3}}, & k\eta \gg 1,\end{cases} \tag{51b}$$

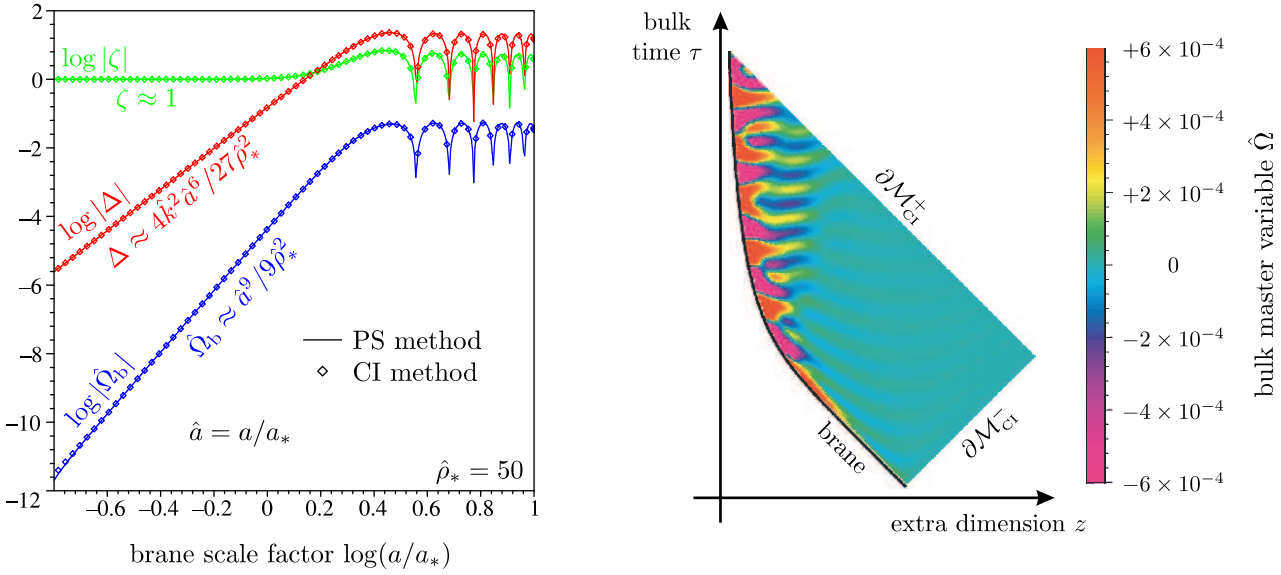

FIG. 2: Comparison between typical results of the PS and CI codes for various brane quantities (*left*); and the typical behaviour of the bulk master variable (*right*) as calculated by the CI method. Very good agreement between the two different numerical schemes is seen in the left panel, despite the fact that they use different initial conditions. We also see excellent consistency between the simulations and the approximations developed in §III D for the behaviour of the system on high-energy/superhorizon scales [c.f. Eqs. (40)–(42)]. Also note that on subhorizon scales, Δ and ζ undergo simple harmonic oscillations, which is consistent with the behaviour in GR (51). The bulk profile demonstrates our choice of initial conditions: We see that the bulk master variable $\hat{\Omega}$ is essentially zero during the early stages of the simulation, and only becomes "large" when the mode crosses the horizon.

where $\mathcal{A}$ is a constant.

In Fig. 3, we show the simulated behaviour of several different gauge invariants on the brane for given subcritical ($k = 0.25k_c$) and supercritical ($k = 10k_c$) modes. These plots illustrate several points that are generic to all of our simulations: The curvature perturbations $\mathcal{R}_c$ and ζ are conserved on superhorizon scales for all cases, just as in general relativity. This useful fact allows us to define the primordial amplitude of a given perturbation as the value of ζ or $\mathcal{R}_c$ before horizon crossing. For the metric perturbations Φ and Ψ, we find that for supercritical and superhorizon scales

$$|\Psi| \gg |\Phi|, \quad \Psi \approx -4\zeta = \text{constant}, \quad (\text{for } a \lesssim a_c \text{ and } k \lesssim Ha). \tag{52}$$

This implies that the Weyl anisotropic stress $\kappa_4^2 \delta\pi_{\mathcal{E}} \approx -\Psi/a^2$ is relatively large in the high-energy superhorizon regime.

Finally, Fig. 4 illustrates how the ordinary superhorizon behaviour of perturbations in GR is recovered for modes entering the Hubble horizon in the low energy era. We see how Δ, Φ and Ψ smoothly interpolate between the non-standard high-energy behaviour to the usual expectations given by (43). Also shown in this plot is the behaviour of the KK anisotropic stress, which steadily decays throughout the simulation. This is characteristic of all the cases we have studied.

C. Enhancement factors and the transfer function

If we examine the curvature perturbations plots in Fig. 3 in detail, we see that the amplitude of ζ increases during horizon crossing. Furthermore, the degree of enhancement seems to increase with increasing k. This is quite different from the behaviour of the perturbations of a radiation dominated universe in ordinary GR (51), where the asymptotic amplitude of ζ is the same before and after horizon crossing. Hence, in the braneworld case we see an enhancement in the amplitude of perturbations that is not present in conventional theory.

What is responsible for this enhancement? As discussed in the Introduction, there are actually two separate effects to consider: First, there is the modification of the universe's expansion at high energies and the $\mathcal{O}(\rho/\sigma)$ corrections to the perturbative equations of motion (30)–(33). Second, there is the effect of the bulk degrees of freedom encapsulated by the bulk master variable Ω (or, equivalently, the KK fluid variables $\Delta_{\mathcal{E}}$, $V_{\mathcal{E}}$ and $\delta\pi_{\mathcal{E}}$). To separate out the two

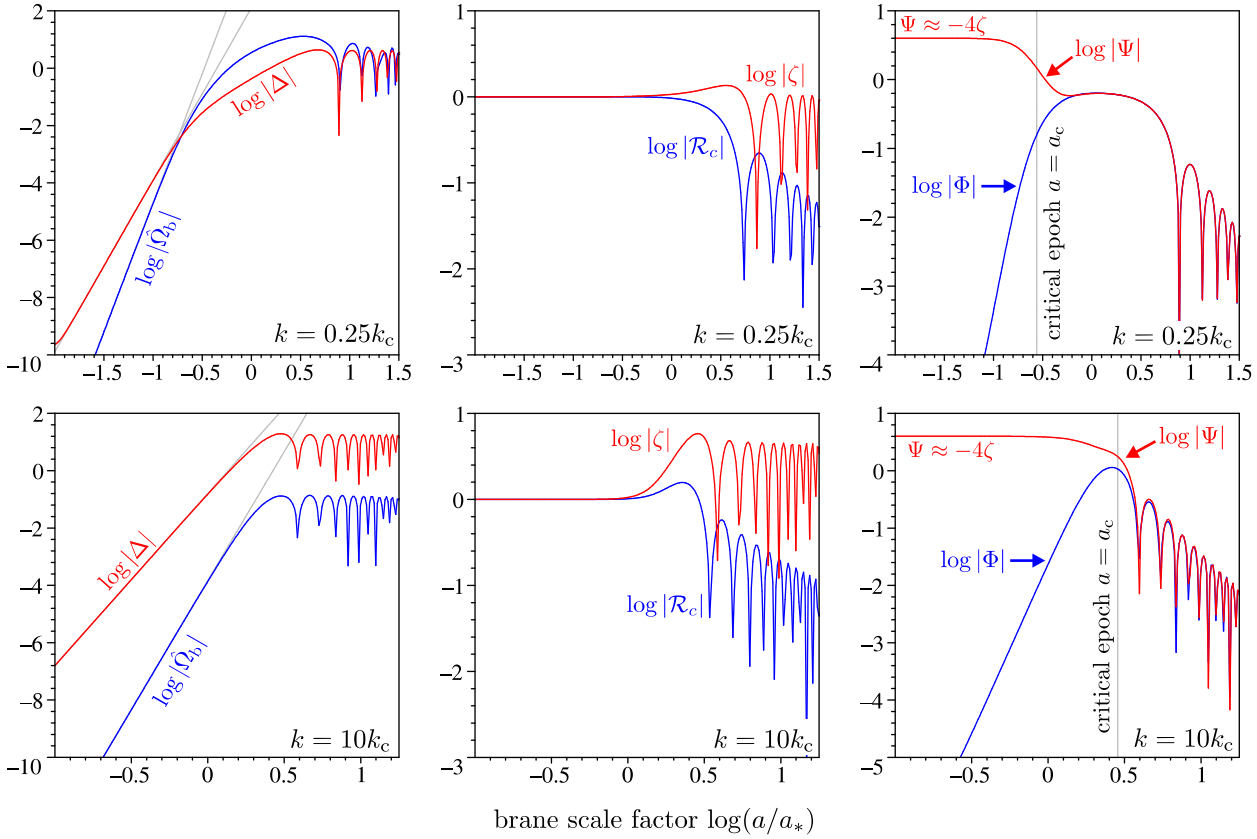

FIG. 3: Typical behaviour of various brane gauge invariants for modes entering the horizon in subcritical (*upper panels*) and supercritical (*lower panels*) epochs. For the plots on the left, the grey straight lines give the analytic expectations (40) for the behaviour of Δ and $\hat{\Omega}_{\rm b}$ on large scales and high energies. The central plots show the comoving and uniform density curvature perturbations, $\mathcal{R}_c$ and ζ respectively. As in conventional cosmology, these are conserved and equal on superhorizon scales. Also note that the amplitude of ζ after horizon crossing is larger for the mode with larger k. The plots on the right show the two gauge invariant metric perturbations on the brane. Before the critical epoch we have that $|\Psi| \gg |\Phi|$, while afterwards we recover the GR result $\Phi \approx -\Psi$. Finally, in the high-energy regime we see $\Psi \approx -4\zeta$, in line with the approximation (41).

effects, it is useful to introduce the 4-dimensional effective theory discussed above where all $\mathcal{O}(\rho/\sigma)$ corrections to GR are retained, but the bulk effects are removed by artificially setting $\Omega = 0$. In the case of radiation domination, we obtain equations for the effective theory density contrast $\Delta_{\rm eff}$ and curvature perturbation $\zeta_{\rm eff}$ from (31) and (33) with $\Omega_{\rm b} = 0$:

$$0 = \frac{d^2\Delta_{\rm eff}}{d\eta^2} + \left(\frac{k^2}{3} - \frac{4\rho a^2}{\sigma\ell^2} - \frac{18\rho^2 a^2}{\sigma^2\ell^2}\right)\Delta_{\rm eff}, \tag{53a}$$

$$\zeta_{\rm eff} = \left(\frac{1}{4} + \frac{3\rho a^2}{2\sigma k^2\ell^2} + \frac{9\rho^2 a^2}{4\sigma^2 k^2\ell^2}\right)\Delta_{\rm eff} + \frac{3Ha}{4k}\frac{d\Delta_{\rm eff}}{d\eta}. \tag{53b}$$

These in conjunction with the Friedmann equation (10) and the conservation of stress energy (11) give a closed set of ODEs on the brane that describe all of the $\mathcal{O}(\rho/\sigma)$ corrections to GR.

In Fig. 5, we plot the predictions of GR, the effective theory, and the full 5-dimensional simulations for the behaviour of ζ and Δ for a supercritical mode. Since in any given model we expect the primordial value of the curvature perturbation to be fixed by inflation, it makes physical sense to normalize the waveforms from each theory such that

$$\zeta_{\rm 5D} \approx \zeta_{\rm eff} \approx \zeta_{\rm GR} \approx 1, \quad a \ll a_*. \tag{54}$$

When this is enforced we see that the effective theory predicts a larger final amplitude for the density perturbation than GR. Furthermore, the final amplitude in the 5-dimensional simulation is larger than both of the other theories. From this we can infer that both $\mathcal{O}(\rho/\sigma)$ and KK effects induce enhancement in the amplitude of perturbations.

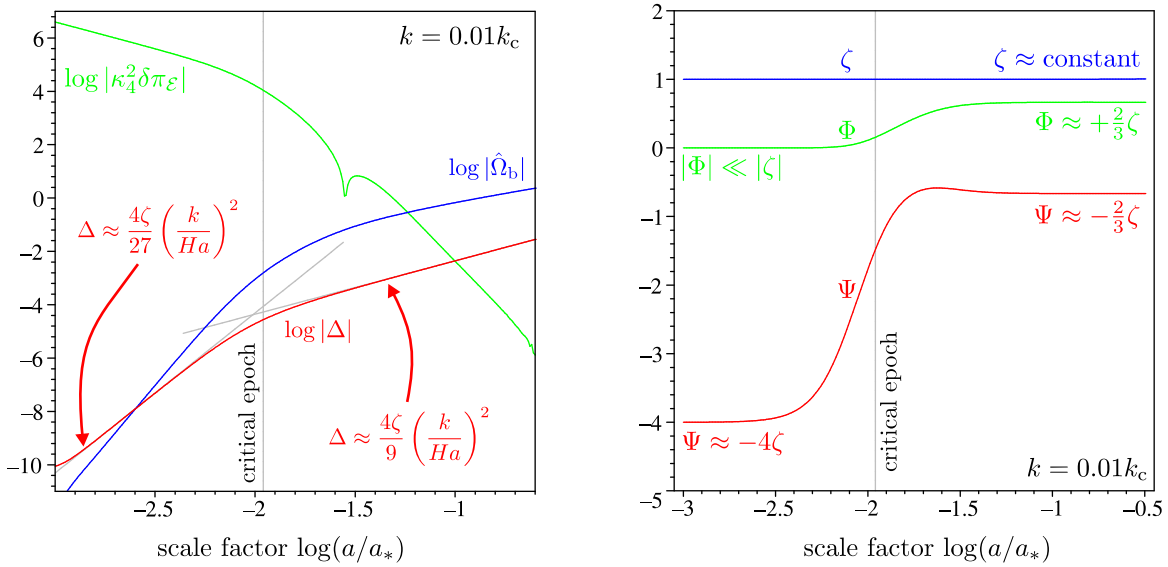

FIG. 4: The simulated behaviour of an extremely subcritical $k \ll k_c$ mode on superhorizon scales. On the left we show how the Δ gauge invariant switches from the high-energy behaviour predicted in Eq. (42) to the familiar GR result (43) as the universe expands through the critical epoch. We also show how the KK anisotropic stress $\kappa_4^2\delta\pi_\mathcal{E}$ steadily decays throughout the simulation, which is typical of all the cases we have investigated. On the right, we show the metric perturbations Φ and Ψ as well as the curvature perturbation ζ. Again, note how the GR result $\Phi \approx -\Psi \approx -2\zeta/3$ is recovered at low energy.

This is in contrast to the situation for tensor perturbations in the Randall-Sundrum model, where modification of the expansion serves to increase the amplitude of gravitational waves while the bulk effects tend to decrease it [28, 29, 31, 32, 33, 34, 35].

The amount of enhancement should be a function of the frequency of the mode, since we expect extremely subcritical modes $k \ll k_c$ to behave as in GR. To test this, we can define a set of "enhancement factors", which are functions of k that describe the relative amplitudes of Δ after horizon crossing in the various theories. As in Fig. 5, let the final amplitudes of the density perturbation with wavenumber k be $\mathcal{C}_{5D}(k)$, $\mathcal{C}_{eff}(k)$ and $\mathcal{C}_{GR}(k)$ for the 5-dimensional, effective and GR theories, respectively, given that the normalization (54) holds. Then, we define enhancement factors as

$$\mathcal{Q}_{eff}(k) = \frac{\mathcal{C}_{eff}(k)}{\mathcal{C}_{GR}(k)}, \quad \mathcal{Q}_\mathcal{E}(k) = \frac{\mathcal{C}_{5D}(k)}{\mathcal{C}_{eff}(k)}, \quad \mathcal{Q}_{5D}(k) = \frac{\mathcal{C}_{5D}(k)}{\mathcal{C}_{GR}(k)}. \tag{55}$$

It follows that $\mathcal{Q}_{eff}(k)$ represents the $\mathcal{O}(\rho/\sigma)$ enhancement to the density perturbation, $\mathcal{Q}_\mathcal{E}(k)$ gives the magnification due to KK modes, while $\mathcal{Q}_{5D}(k)$ gives the total 5-dimensional amplification over the GR case. These enhancement factors are shown in the left panel of Fig. 6. We can see that they all increase as the scale is decreased, and that they all approach unity for $k \to 0$. Since $\mathcal{Q} = 1$ implies no enhancement of the density perturbations over the standard result, this means we recover general relativity on large scales. For all wavenumbers we see $\mathcal{Q}_{eff} > \mathcal{Q}_\mathcal{E} > 1$, which implies that the amplitude magnification due to the $\mathcal{O}(\rho/\sigma)$ corrections is always larger than that due to the KK modes. Interestingly, the $\mathcal{Q}$-factors appear to approach asymptotically constant values for large k:

$$\mathcal{Q}_{eff}(k) \approx 3.0, \quad \mathcal{Q}_\mathcal{E}(k) \approx 2.4, \quad \mathcal{Q}_{5D}(k) \approx 7.1, \quad k \gg k_c. \tag{56}$$

It is difficult to know if these are the true asymptotic limits for $k \to \infty$ due to the limitations of computing power.

In cosmological perturbation theory, transfer functions are very important quantities. They allow one to transform the primordial spectrum of some quantity set during inflation into the spectrum of another quantity at a later time. In this sense, they are essentially the Fourier transform of the retarded Green's function for cosmological perturbations. There are many different transfer functions one can define, but for our case it is useful to consider a function $T(k)$ that will tell us how the initial spectrum of curvature perturbations $\mathcal{P}_\zeta^{inf}$ maps onto the spectrum of density perturbations $\mathcal{P}_\Delta$ at some low energy epoch within the radiation era characterized by the conformal time $\eta > \eta_c$. It is customary

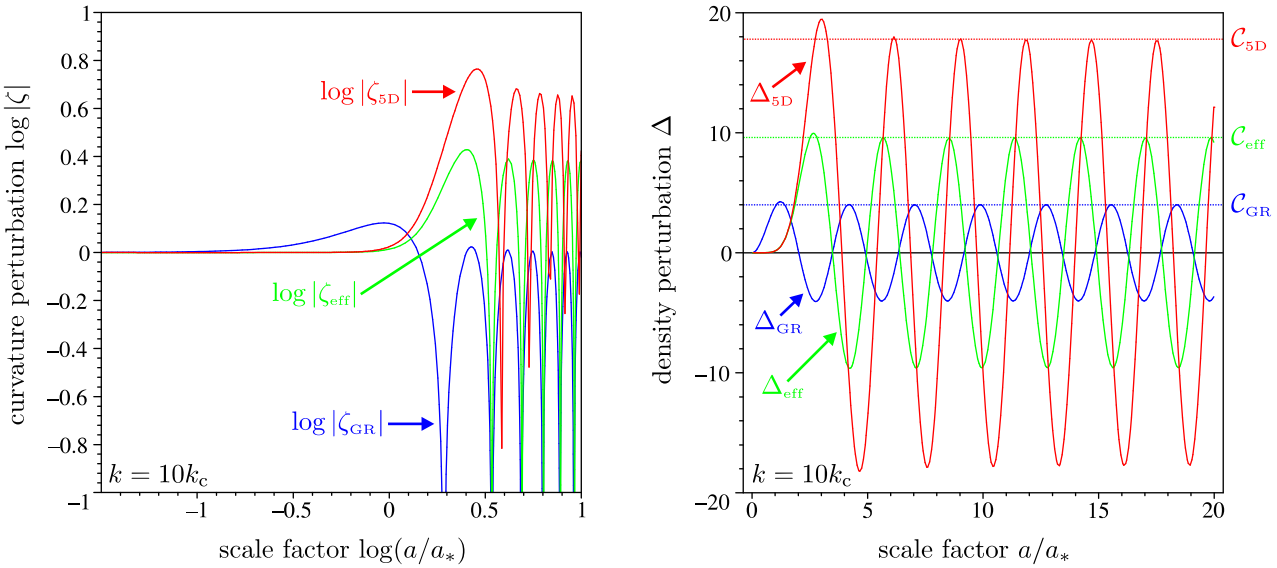

FIG. 5: A comparison of the behaviour of the curvature perturbation ζ (*left*) and the density perturbation Δ (*right*) in the full 5-dimensional theory including KK contributions (5D), the effective 4-dimension theory including $\mathcal{O}(\rho/\sigma)$ corrections (eff), and ordinary general relativity (GR). The waveforms for each theory are normalized such that $\zeta = 1$ on superhorizon scales. We can clearly see that given the same primordial values of the curvature perturbation, the final amplitude of the density perturbation in the 5D theory $\mathcal{C}_{5D}$ is larger than in the effective theory $\mathcal{C}_{\rm eff}$, which in turn is larger than the GR value $\mathcal{C}_{\rm GR} = 4$.

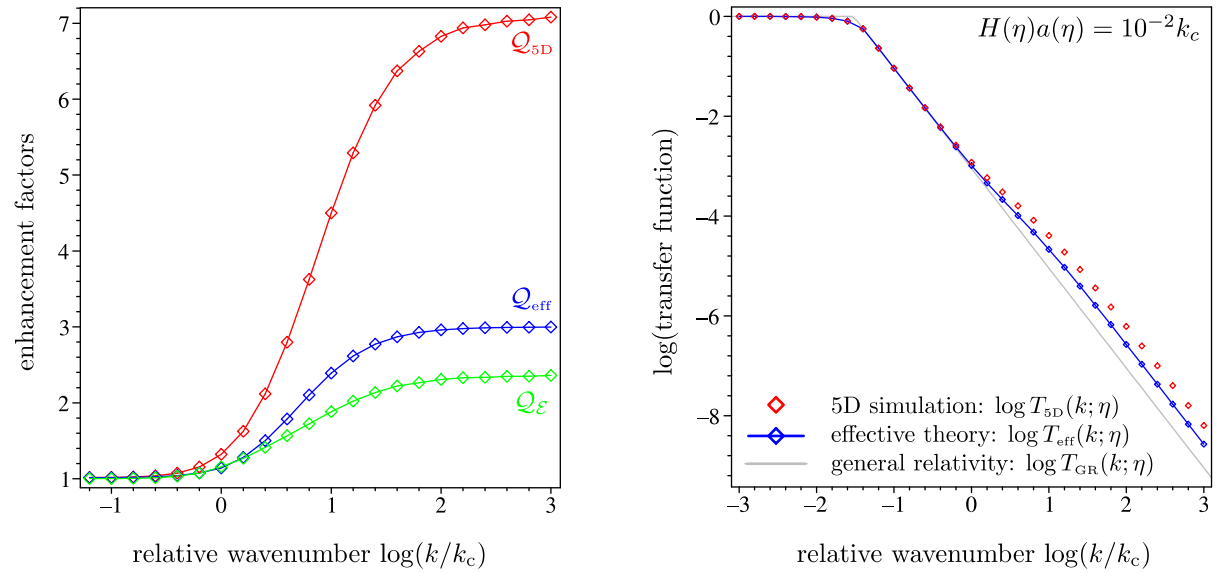

FIG. 6: Density perturbation enhancement factors (*left*) and transfer functions (*right*) from simulations, effective theory, and general relativity. All of the $\mathcal{Q}$ factors monotonically increase with k/k_c, and we see that the Δ amplitude enhancement due to $\mathcal{O}(\rho/\sigma)$ effects $\mathcal{Q}_{\rm eff}$ is generally larger than the enhancement due to KK effects $\mathcal{Q}_{\mathcal{E}}$. For asymptotically small scales $k \gg k_c$, the enhancement seems to level off. The transfer functions in the right panel are evaluated at a given subcritical epoch in the radiation dominated era. The T functions show how, for a fixed primordial spectrum of curvature perturbations $\mathcal{P}_\zeta^{\rm inf}$, the effective theory predicts excess power in the Δ spectrum $\mathcal{P}_\Delta \propto T^2 \mathcal{P}_\zeta^{\rm inf}$ on supercritical/subhorizon scales compared to the GR result. The excess small-scale power is even greater when KK modes are taken into account, as shown by $T_{5D}(k;\eta)$.

to normalize transfer functions such that $T(k;\eta) \xrightarrow[0]{k} 1$, which leads us to the following definition

$$T(k;\eta) = \frac{9}{4}\left[\frac{k}{H(\eta)a(\eta)}\right]^{-2}\frac{\Delta_k(\eta)}{\zeta_k^{\rm inf}}. \tag{57}$$

Here, $\zeta_k^{\rm inf}$ is the primordial value of the curvature perturbation and $\Delta_k(\eta)$ is the maximum amplitude of the density perturbation in the epoch of interest. As demonstrated in Fig. 4, we know that we recover the GR result in the extreme small scale limit

$$\Delta_k(\eta) \xrightarrow[0]{k} \frac{4}{9}\left[\frac{k}{H(\eta)a(\eta)}\right]^{2}\zeta_k^{\rm inf}, \quad (a > a_c), \tag{58}$$

which gives the transfer function the correct normalization. In GR, the transfer function is accurately given by

$$T_{\rm GR}(k;\eta) \approx \begin{cases} 1, & k < 3Ha, \\ (3Ha/k)^2, & k > 3Ha. \end{cases} \tag{59}$$

In the righthand panel of Fig. 6, we show the transfer functions derived from GR, the effective theory and the 5-dimensional simulations. As expected, the $T(k;\eta)$ for each formulation match one another on subcritical scales $k < k_{\rm c}$. However, on supercritical scales we have $T_{\rm 5D} > T_{\rm eff} > T_{\rm GR}$.

Note that if we are interested in the transfer function at some arbitrary epoch in the low-energy radiation regime $Ha \gg k_c$, it is approximately given in terms of the enhancement factor as follows:

$$T_{\rm 5D}(k;\eta) \approx \begin{cases} 1, & k < 3Ha, \\ (3Ha/k)^2\mathcal{Q}_{\rm 5D}(k), & k > 3Ha, \end{cases} \tag{60}$$

Now, the spectrum of density fluctuations at any point in the radiation era is given by

$$\mathcal{P}_\Delta(k;\eta) = \frac{16}{81}T^2(k;\eta)\left(\frac{k}{Ha}\right)^4\mathcal{P}_\zeta^{\rm inf}(k). \tag{61}$$

Using the enhancement factor results in Fig. 6 with Eqns. (59) and (60), we see that the RS matter power spectrum (evaluated in the low-energy regime) is ~ 50 times bigger than the GR prediction on supercritical scales $k \sim 10^3 k_{\rm c}$.

D. Alternate initial data

Before concluding, we wish to briefly revisit the issue of initial conditions. We have argued above that the existence of a dominant growing mode at high-energy and on superhorizon scales means that the details of initial data for our simulations are unimportant. To some degree, the fact that the PS and CI algorithms produce essentially identical results is a good confirmation of this, since each method uses a different prescription for initial data.

But what if we were to use different classes of initial data? For example, we could modify the CI initial data such that the bulk field has constant amplitude along the initial data surface:

$$\hat{\Omega}(\partial\mathcal{M}^-_{\rm CI}) = \hat{\Omega}_i = \text{constant}. \tag{62}$$

The waveforms generated by such a choice are shown in Fig. 7. Though the overall amplitude and early time behaviour of the signal seems to be sensitive to the initial value of $\hat{\Omega}$, the ratio of the final amplitude of Δ to the initial value of ζ is the same for each choice of initial data. We have confirmed that this is also true for other choices of $\hat{\Omega}(\partial\mathcal{M}^-_{\rm CI})$, including the case when the initial data is a simple sinusoid.[4] Ultimately, it is the ratio $\Delta(k\eta \gg 1)/\zeta(k\eta \ll 1)$ that is relevant to the transfer function used to transcribe the predictions of inflation into observable quantities, hence we can be confident that our principal results hold for reasonable modifications of initial data.

[4] Sinusoidal initial data was used in Ref. [35] to test the insensitivity of the final spectrum of the stochastic background of gravitational waves to initial conditions in RS models.

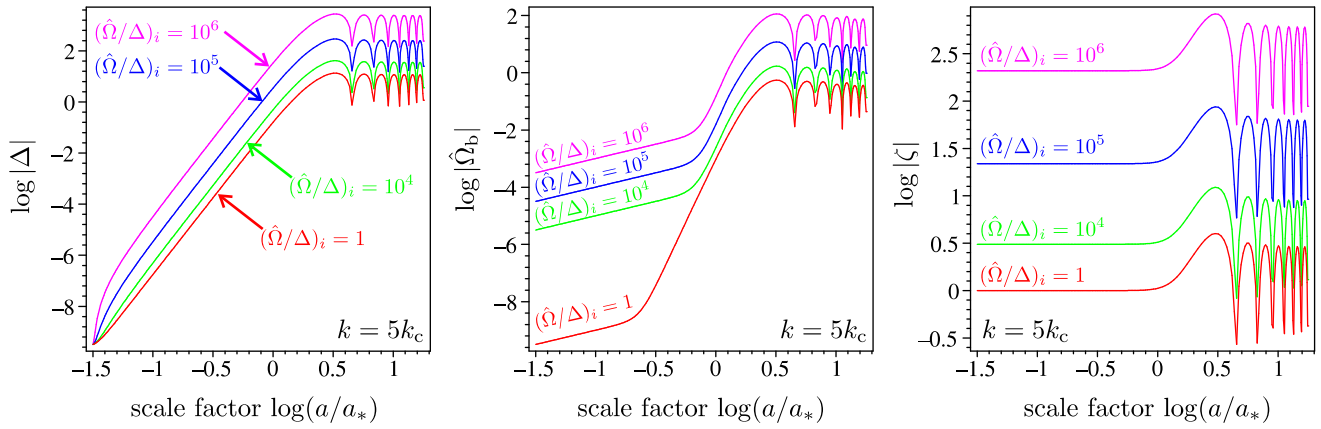

FIG. 7: Simulated waveforms for $\hat{\Omega}$ = constant initial data in the CI method. Here, $(\hat{\Omega}/\Delta)_i$ is the ratio of the bulk field to the density perturbation at the initial time; this ratio is zero for the other simulations in this paper. The early time behaviour of Δ and $\hat{\Omega}_b$ shows some sensitivity to $(\hat{\Omega}/\Delta)_i$, but otherwise the waveforms are identical to one another up to an overall amplitude scaling. Indeed, if we normalize the simulation results by the initial value of ζ we find that all of the Δ waveforms are coincident at late times, which means that the enhancement factor $\mathcal{Q}_{5D}$ and transfer function T_{5D} are insensitive to $(\hat{\Omega}/\Delta)_i$. Note that at early times we have $\hat{\Omega}_b \propto a$, which matches the behaviour of the subdominant growing mode from Eq. (40). This confirms our expectations: varying the initial data causes the other subdominant modes to be excited to various degrees, but the dominant growing mode always "wins" at late times.

V. DISCUSSION AND IMPLICATIONS

In this paper, we have written down the equations of motion for generic gauge-invariant scalar cosmological perturbations in the RS braneworld model in a form suitable for numeric analysis (§III). We have developed new analytic approximations for the behaviour of fluctuations on high-energy superhorizon scales (§III D) for a radiation dominated brane. We have applied two different numerical algorithms to solve the equations in the early radiation-dominated universe (§IV). Our numerical results show that the amplitude of modes which enter the Hubble horizon during the high-energy regime gets enhanced over the the standard GR result. Conversely, modes which enter at low energy do not show any late-time deviations from standard theory, as seen in Fig. 4. We only recover standard results for the metric perturbations, such as $\Psi \approx -\Phi$, at low energies.

Our simulations confirm the common sense expectation that all tangible effects from the fifth dimension are on scales smaller than a critical value k_c^{-1}, whose physical size today is given by Eq. (47). To parameterize the degree of amplification as a function of scale, we introduced so-called "enhancement factors" and transfer functions in §IV C. These show that the degree of enhancement over the GR case seems to reach a constant value at high k; the amplification of the subhorizon matter power spectrum is ~ 50 for $k \sim 10^3 k_c$. We presented analytic arguments and numerical evidence that our results are robust against modifications of the initial data for simulations (§IV D).

As discussed in §I and §IV C, the enhancement of perturbations upon horizon crossing can be attributed to two effects: namely, the $\mathcal{O}(\rho/\sigma)$ corrections to the background dynamics and the influence of the KK modes. Both of these give roughly equal contributions to the enhancement (Fig. 6). One could have anticipated the KK enhancement on simple physical grounds by arguing as follows: In Ref. [37] it was shown that the gravitational force of attraction between two bodies in the RS one brane model is

$$\text{gravitational force} \sim \begin{cases} \kappa_4^2/r^2, & r \gg \ell, \\ \kappa_5^2/r^3 = \kappa_4^2 \ell/r^3, & r \ll \ell. \end{cases} \tag{63}$$

That is, the Newtonian force becomes 5-dimensional on small scales. This implies that the gravitational force is stronger than usual on scales $r \lesssim \ell$. It then follows that the self-gravity of perturbative modes that enter the horizon at high energies $H\ell \gtrsim 1$ will be greater than those which enter at low energies $H\ell \lesssim 1$. Therefore, we should expect that the amplitude of small-scale modes to be magnified over the amplitude of large-scale modes during horizon crossing in braneworld cosmology, which is exactly what we have seen in our simulations.[5]

[5] However, we should note that this simple argument neglects the influence of the KK anisotropic stress, which we know is non-negligible

The amplitude enhancement of perturbations is important on comoving scales $\lesssim 10\,\mathrm{AU}$, which are far too small to be relevant to present-day/cosmic microwave background measurements of the matter power spectrum. However, it may have an important bearing on the formation of compact objects such as primordial black holes and boson stars at very high energies, i.e. the greater gravitational force of attraction in the early universe will create more of these objects than in GR (different aspects of primordial black holes in RS cosmology in the context of various effective theories have been considered in Refs. [41, 42, 43, 44, 45, 46, 47]). We know that the abundance of primordial black holes can be constrained by big bang nucleosythesis and observations of high-energy cosmic rays, so it would be interesting to see if the kind of enhancement of density perturbations predicted in this paper can be used to derive new limits on Randall-Sundrum cosmology. We leave this issue for future work.

Acknowledgments

AC is supported by FCT (Portugal) PhD fellowship SFRH/BD/19853/2004. KK and SSS are supported by PPARC (UK).

[1] L. Randall and R. Sundrum, Phys. Rev. Lett. **83**, 4690 (1999), hep-th/9906064.
[2] D. Langlois, Prog. Theor. Phys. Suppl. **148**, 181 (2003), hep-th/0209261.
[3] R. Maartens, Living Rev. Rel. **7**, 7 (2004), gr-qc/0312059.
[4] P. Brax, C. van de Bruck, and A.-C. Davis, Rept. Prog. Phys. **67**, 2183 (2004), hep-th/0404011.
[5] D. J. Kapner et al., Phys. Rev. Lett. **98**, 021101 (2007), hep-ph/0611184.
[6] S. Mukohyama, Phys. Rev. **D62**, 084015 (2000), hep-th/0004067.
[7] H. Kodama, A. Ishibashi, and O. Seto, Phys. Rev. **D62**, 064022 (2000), hep-th/0004160.
[8] C. van de Bruck, M. Dorca, R. H. Brandenberger, and A. Lukas, Phys. Rev. **D62**, 123515 (2000), hep-th/0005032.
[9] K. Koyama and J. Soda, Phys. Rev. **D62**, 123502 (2000), hep-th/0005239.
[10] D. Langlois, Phys. Rev. Lett. **86**, 2212 (2001), hep-th/0010063.
[11] K. Koyama, D. Langlois, R. Maartens, and D. Wands, JCAP **0411**, 002 (2004), hep-th/0408222.
[12] K. Koyama, S. Mizuno, and D. Wands, JCAP **0508**, 009 (2005), hep-th/0506102.
[13] T. Hiramatsu and K. Koyama, JCAP **0612**, 009 (2006), hep-th/0607068.
[14] C. de Rham and S. Watson (2007), hep-th/0702048.
[15] K. Koyama, A. Mennim, V. A. Rubakov, D. Wands, and T. Hiramatsu (2007), hep-th/0701241.
[16] C. Gordon and R. Maartens, Phys. Rev. **D63**, 044022 (2001), hep-th/0009010.
[17] D. Langlois, R. Maartens, M. Sasaki, and D. Wands, Phys. Rev. **D63**, 084009 (2001), hep-th/0012044.
[18] P. Brax, C. van de Bruck, and A. C. Davis, JHEP **10**, 026 (2001), hep-th/0108215.
[19] H. A. Bridgman, K. A. Malik, and D. Wands, Phys. Rev. **D65**, 043502 (2002), astro-ph/0107245.
[20] K. Koyama and J. Soda, Phys. Rev. **D65**, 023514 (2002), hep-th/0108003.
[21] B. Leong, P. Dunsby, A. Challinor, and A. Lasenby, Phys. Rev. **D65**, 104012 (2002), gr-qc/0111033.
[22] B. Leong, A. Challinor, R. Maartens, and A. Lasenby, Phys. Rev. **D66**, 104010 (2002), astro-ph/0208015.
[23] R. Easther, D. Langlois, R. Maartens, and D. Wands, JCAP **0310**, 014 (2003), hep-th/0308078.
[24] R. A. Battye, C. Van de Bruck, and A. Mennim, Phys. Rev. **D69**, 064040 (2004), hep-th/0308134.
[25] T. Kobayashi and T. Tanaka, JCAP **0410**, 015 (2004), gr-qc/0408021.
[26] R. A. Battye and A. Mennim, Phys. Rev. **D70**, 124008 (2004), hep-th/0408101.
[27] K. Koyama, JCAP **0409**, 010 (2004), astro-ph/0407263.
[28] T. Hiramatsu, K. Koyama, and A. Taruya, Phys. Lett. **B578**, 269 (2004), hep-th/0308072.
[29] T. Hiramatsu, K. Koyama, and A. Taruya, Phys. Lett. **B609**, 133 (2005), hep-th/0410247.
[30] T. Hiramatsu, Phys. Rev. **D73**, 084008 (2006), hep-th/0601105.
[31] T. Kobayashi and T. Tanaka, Phys. Rev. **D73**, 044005 (2006), hep-th/0511186.
[32] T. Kobayashi and T. Tanaka, Phys. Rev. **D71**, 124028 (2005), hep-th/0505065.
[33] T. Kobayashi, Phys. Rev. **D73**, 124031 (2006), hep-th/0602168.
[34] K. Ichiki and K. Nakamura, Phys. Rev. **D70**, 064017 (2004), hep-th/0310282.
[35] S. S. Seahra, Phys. Rev. **D74**, 044010 (2006), hep-th/0602194.
[36] A. Cardoso, K. Koyama, A. Mennim, S. S. Seahra, and D. Wands (2006), hep-th/0612202.
[37] J. Garriga and T. Tanaka, Phys. Rev. Lett. **84**, 2778 (2000), hep-th/9911055.
[38] H. Kodama and M. Sasaki, Prog. Theor. Phys. Suppl. **78**, 1 (1984).

at high energies.

[39] T. Shiromizu, K.-i. Maeda, and M. Sasaki, Phys. Rev. **D62**, 024012 (2000), gr-qc/9910076.
[40] C. Deffayet, Phys. Rev. **D66**, 103504 (2002), hep-th/0205084.
[41] Y. Sendouda, S. Nagataki, and K. Sato, JCAP **0606**, 003 (2006), astro-ph/0603509.
[42] R. Guedens, D. Clancy, and A. R. Liddle, Phys. Rev. **D66**, 043513 (2002), astro-ph/0205149.
[43] R. Guedens, D. Clancy, and A. R. Liddle, Phys. Rev. **D66**, 083509 (2002), astro-ph/0208299.
[44] A. S. Majumdar, Phys. Rev. Lett. **90**, 031303 (2003), astro-ph/0208048.
[45] D. Clancy, R. Guedens, and A. R. Liddle, Phys. Rev. **D68**, 023507 (2003), astro-ph/0301568.
[46] Y. Sendouda, S. Nagataki, and K. Sato, Phys. Rev. **D68**, 103510 (2003), astro-ph/0309170.
[47] Y. Sendouda, K. Kohri, S. Nagataki, and K. Sato, Phys. Rev. **D71**, 063512 (2005), astro-ph/0408369.